Appendix A. Model convergence

Figure A.1: Trace plots for the logistic basis parameters $\pi_k a_{kz}, b_k$, parameters of the unstructured covariance matrix $\Lambda C \Lambda$, and prior scale parameters σ_γ and σ_α. Different colors correspond to different biomarkers (i.e., $k = 1, 2, \ldots, K = 9$). Plots on the left show the distribution of all samples, and plots on the right show the sampled values at each iteration.
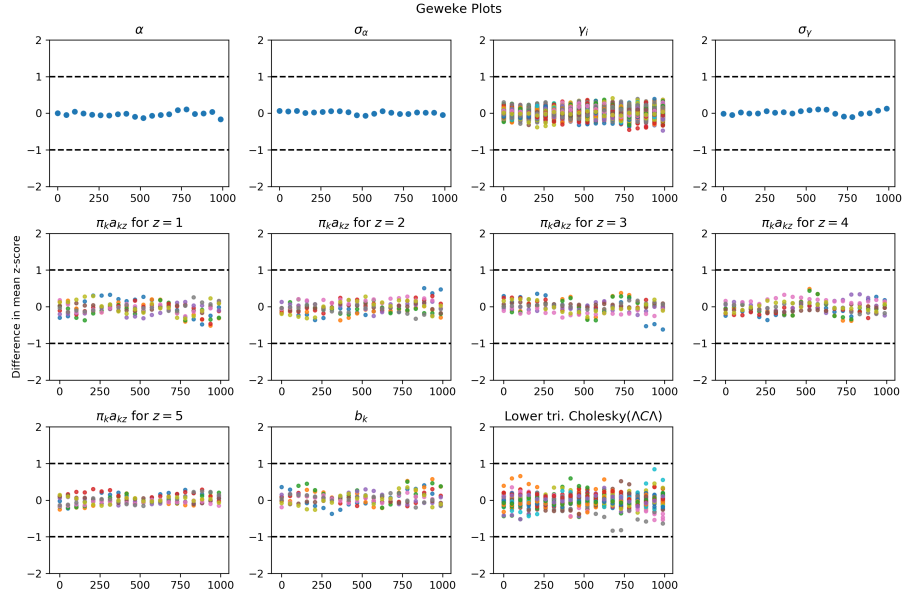
Figure A.2: Geweke plots (comparing mean of the first 10% and mean of the last 50% of chain, computed in 20 segments) for the logistic basis parameters $\pi_k a_{kz}, b_k$, parameters of the unstructured covariance matrix $\Lambda C \Lambda$, prior scale parameters σ_γ and σ_α, and subject-specific initial point estimates γ_i. Different colors correspond to different biomarkers (i.e., $k = 1, 2, \ldots, K = 9$) or different subjects (i.e., $i = 1, 2, \ldots, n = 1369$). Values remain between -1 and +1, as required for a chain that has converged.

Appendix B. Simulation experiments

We conducted simulation experiments to evaluate recovery of model parameters and to assess model sensitivity to pre-specified hyperprior parameters. First, we fixed "ground truth" values for all model parameters and generated biomarker observations to construct a simulated longitudinal data set for 100 subjects with 9 biomarkers. Next, blinded to all "ground truth" values except for the scale parameters of the hyperpriors on σ_α and σ_γ, we fitted the model. In the first experiment, hyperprior parameters were fixed at their ground truth values. The goal of this experiment was to assess the recovery of true γ values and biomarker trajectories. The Pearson correlation between true and estimated γ values was 0.9897 (Fig. B.3), and the estimated biomarker trajectories closely resembled the true trajectories (Fig. B.4).
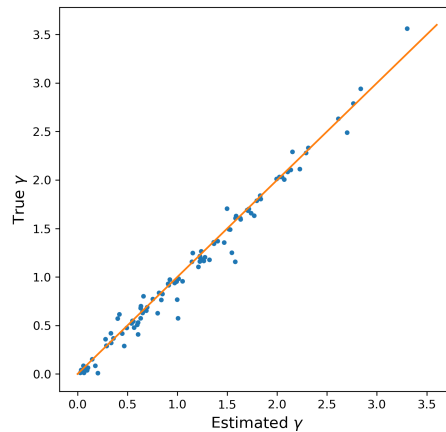

Figure B.3: True vs. estimated γ values in the first simulation experiment.

In the following experiments, we used different values for the scale parameters of the half-$\mathcal{N}$ hyperpriors on σ_α and σ_γ to fit the model. We computed the Pearson correlation between estimated γ_i's and their true values for each experiment (Fig. B.5). For each biomarker, we also computed the similarity between true and estimated trajectories as the maximum vertical distance between the curves in the domain of true progression scores (Fig. B.6). Results showed that unless the scale parameters of the half-$\mathcal{N}$ hyperpriors on σ_α and σ_γ are fixed at very small values, resulting in a very restrictive hyperprior, misspecification of these hyperprior parameters does not significantly affect model performance.
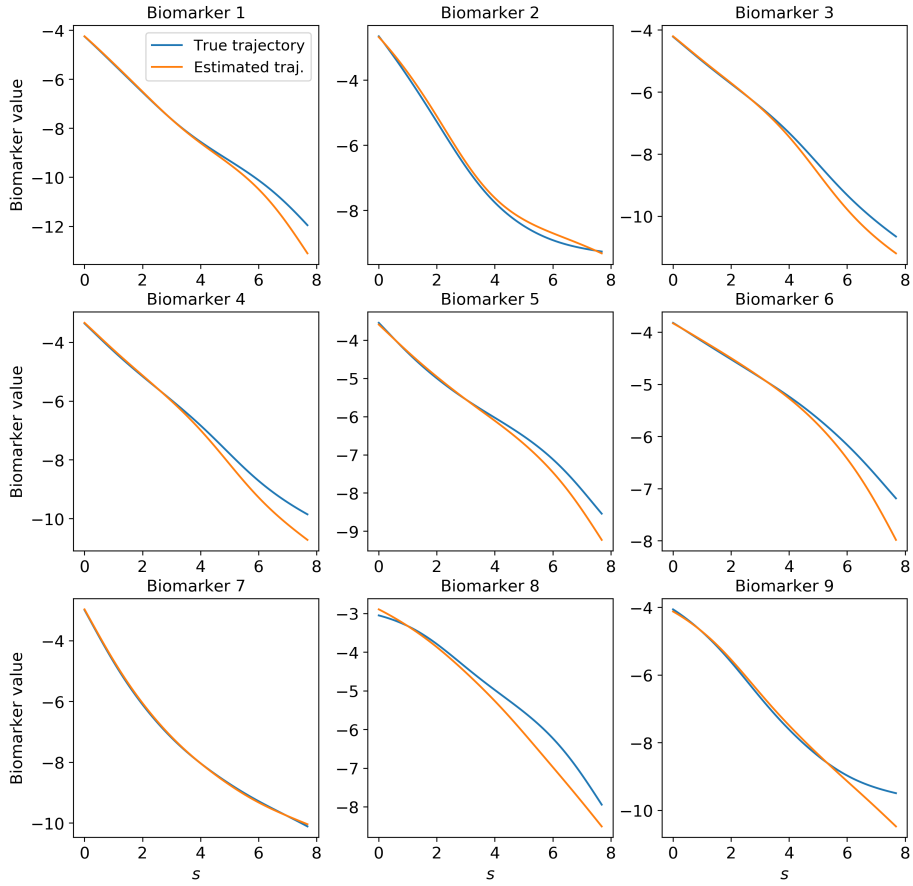
Figure B.4: True (blue) and estimated (orange) biomarker trajectories in the first simulation experiment.
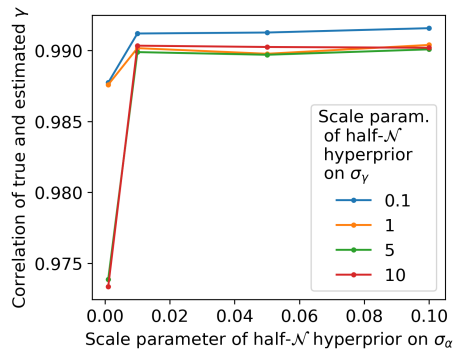

Figure B.5: Pearson correlation between true and estimated γ values for different values of scale parameters of the half-$\mathcal{N}$ hyperpriors on σ_α and σ_γ.
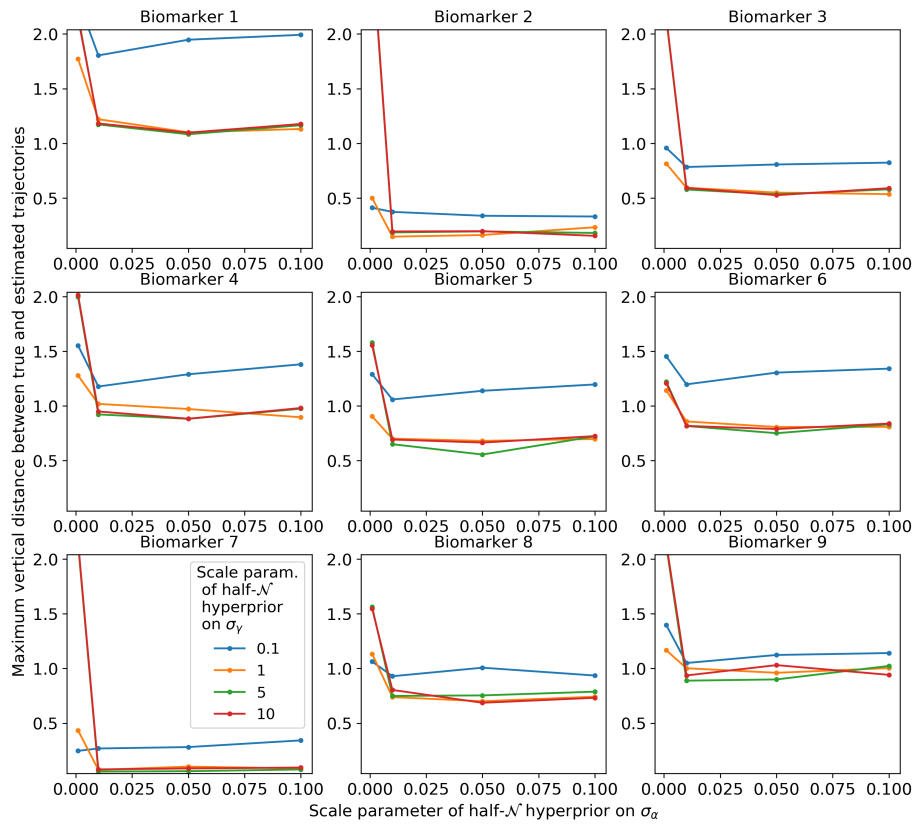
21

Figure B.6: Maximum vertical distance between true and estimated biomarker trajectories for different values of scale parameters of the half-$\mathcal{N}$ hyperpriors on σ_α and σ_γ.

Appendix C. Comparison to existing models of disease progression

We compared the performance of PS in predicting time to dementia onset to the performance of similar measures obtained from two previously described models of Alzheimer's disease progression: Latent Time Joint Mixed effects Model (LTJMM) [11] (`https://bitbucket.org/mdonohue/ltjmm`) and Gaussian Process Progression Model (GPPM) [15] (`https://github.com/marcolorenzi/GP_progression_model`). We wrote code as needed for setting up the models and providing data in the required formats, but did not make any changes to the source code provided. We trained the models using the same set of 9 biomarkers. Each of these models estimate a subject-specific time-shift. Adding this time-shift to the baseline age yields the "disease age". We used the disease ages estimated for participants in the training set to train a linear regression model with time to dementia onset from baseline as the outcome and disease age as the independent variable. We then predicted time to dementia onset using this linear regression model and the estimated disease ages for each participant in the testing set.

Appendix C.1. LTJMM

As described by Li et al. [11], we included a fixed effect for age as a time-varying covariate in LTJMM. We did not include any other covariates in order to keep the model similar to ours. Following the same procedure used by Li et al. [11], we ran three parallel Markov chains, using 4000 warm-up + 4000 iterations. We combined the training and testing sets for the purpose of fitting the LTJMM, since a function to estimate the time-shift for individuals not included in training was not provided in the R package. Using the notation of Li et al. [11], disease age was computed as $t_{i,j=0} + \delta_i$ for each individual i in the testing set, where $j = 0$ indicates baseline.

Appendix C.2. GPPM

We followed the approach outlined in the example code provided for ADNI data in the GPPM repository. The function provided for importing data requires that each individual included in analysis have at least one measurement per biomarker. Given the missingness in the data set, particularly for the CSF measures, this requirement reduced the training set to 319 individuals, and the testing set to 85 individuals. We fitted the model using the 319 training individuals, and obtained predictions for the time-shift for each of the 85 testing individuals. For comparison purposes, we report the performance of the PS computed using our proposed model in this smaller testing set. Using the notation of Lorenzi et al. [15], disease age was computed as $\phi^j(\tau) = \tau + d^j$ for each individual j in the testing set, where τ is the age of individual j at baseline.

Appendix C.3. SReFT

We could not run Statistical Restoration of Fragmented Time course (SReFT) [14] using the code provided at `https://bitbucket.org/tokudakeita/sreft`. The example Matlab code was hardcoded for 3 biomarkers, and working with an arbitrary number of biomarkers required substantial changes to the code.

References

1. Villemagne VL, Burnham S, Bourgeat P, Brown B, Ellis KA, Salvado O, Szoeke C, Macaulay SL, Martins R, Maruff P, Ames D, Rowe CC, Masters CL. Amyloid β deposition, neurodegeneration, and cognitive decline in sporadic Alzheimer's disease: a prospective cohort study. *Lancet Neurology* 2013;12(4):357–67. URL: http://www.ncbi.nlm.nih.gov/pubmed/23477989. doi:10.1016/S1474-4422(13)70044-9.

2. Bateman RJ, Xiong C, Benzinger TLS, Fagan AM, Goate A, Fox NC, Marcus DS, Cairns NJ, Xie X, Blazey TM, Holtzman DM, Santacruz A, Buckles V, Oliver A, Moulder K, Aisen PS, Ghetti B, Klunk WE, McDade E, Martins RN, Masters CL, Mayeux R, Ringman JM, Rossor MN, Schofield PR, Sperling RA, Salloway S, Morris JC. Clinical and biomarker changes in dominantly inherited Alzheimer's disease. *New England Journal of Medicine* 2012;367(9):795–804. URL: http://www.pubmedcentral.nih.gov/articlerender.fcgi?artid=3474597{&}tool=pmcentrez{&}rendertype=abstract. doi:10.1056/NEJMoa1202753.

3. Fonteijn HM, Modat M, Clarkson MJ, Barnes J, Lehmann M, Hobbs NZ, Scahill RI, Tabrizi SJ, Ourselin S, Fox NC, Alexander DC. An event-based model for disease progression and its application in familial Alzheimer's disease and Huntington's disease. *NeuroImage* 2012;60(3):1880–9. URL: http://www.ncbi.nlm.nih.gov/pubmed/22281676. doi:10.1016/j.neuroimage.2012.01.062.

4. Young AL, Oxtoby NP, Daga P, Cash DM, Fox NC, Ourselin S, Schott JM, Alexander DC. A data-driven model of biomarker changes in sporadic Alzheimer's disease. *Brain* 2014;137:2564–77. URL: http://www.ncbi.nlm.nih.gov/pubmed/25012224. doi:10.1093/brain/awu176.

5. Oxtoby NP, Young AL, Cash DM, Benzinger TLS, Fagan AM, Morris JC, Bateman RJ, Fox NC, Schott JM, Alexander DC. Data-driven models of dominantly-inherited Alzheimer's disease progression. *Brain* 2018;141(5):1529–44. doi:10.1093/brain/awy050.

6. Jedynak BM, Lang A, Liu B, Katz E, Zhang Y, Wyman BT, Raunig D, Jedynak CP, Caffo B, Prince JL. A computational neurodegenerative disease progression score: Method and results with the Alzheimer's Disease Neuroimaging Initiative cohort. *NeuroImage* 2012;63(3):1478–86. URL: http://www.pubmedcentral.nih.gov/articlerender.fcgi?artid=3472161{&}tool=pmcentrez{&}rendertype=abstract. doi:10.1016/j.neuroimage.2012.07.059.

7. Bilgel M, Prince JL, Wong DF, Resnick SM, Jedynak BM. A multivariate nonlinear mixed effects model for longitudinal image analysis: Application to amyloid imaging. *NeuroImage* 2016;134:658–70. URL: http://dx.doi.org/

10.1016/j.neuroimage.2016.04.001. doi:10.1016/j.neuroimage.2016.04.001.

8. Marinescu RV, Eshaghi A, Lorenzi M, Young AL, Oxtoby NP, Garbarino S, Shakespeare TJ, Crutch SJ, Alexander DC. A vertex clustering model for disease progression: Application to cortical thickness images. In: Niethammer M, Styner M, Aylward S, Zhu H, Oguz I, Yap PT, Shen D, eds. *Lecture Notes in Computer Science, Information Processing in Medical Imaging*; vol. 10265. Springer. ISBN 9783319590493; 2017:134–45. doi:10.1007/978-3-319-59050-9_11.

9. Schiratti JB, Allassonniere S, Routier A, Colliot O, Durrleman S. A mixed-effects model with time reparametrization for longitudinal univariate manifold-valued data. In: Ourselin S, Alexander DC, Westin CF, Cardoso MJ, eds. *Lecture Notes in Computer Science, Information Processing in Medical Imaging*; vol. 9123. Springer. ISBN 3-540-54246-9; 2015:564–75. doi:10.1097/00003072-199201000-00023.

10. Donohue MC, Jacqmin-Gadda H, Le Goff M, Thomas RG, Raman R, Gamst AC, Beckett La, Jack CR, Weiner MW, Dartigues JF, Aisen PS. Estimating long-term multivariate progression from short-term data. *Alzheimer's and Dementia* 2014;10(5):S400–10. doi:10.1016/j.jalz.2013.10.003.

11. Li D, Iddi S, Thompson WK, Donohue MC. Bayesian latent time joint mixed effect models for multicohort longitudinal data. *Statistical Methods in Medical Research* 2017;doi:10.1177/0962280217737566. arXiv:1703.10266.

12. Guerrero R, Schmidt-Richberg A, Ledig C, Tong T, Wolz R, Rueckert D. Instantiated mixed effects modeling of Alzheimer's disease markers. *NeuroImage* 2016;142:113–25. URL: http://dx.doi.org/10.1016/j.neuroimage.2016.06.049. doi:10.1016/j.neuroimage.2016.06.049.

13. Koval I, Schiratti JB, Routier A, Bacci M, Colliot O, Allassonnière S, Durrleman S. Spatiotemporal propagation of the cortical atrophy: Population and individual patterns. *Frontiers in Neurology* 2018;9:235. URL: http://journal.frontiersin.org/article/10.3389/fneur.2018.00235/full. doi:10.3389/fneur.2018.00235.

14. Ishida T, Tokuda K, Hisaka A, Honma M, Kijima S, Takatoku H, Iwatsubo T, Moritoyo T, Suzuki H. A novel method to estimate long-term chronological changes from fragmented observations in disease progression. *Clinical Pharmacology & Therapeutics* 2018;:[in press]URL: http://doi.wiley.com/10.1002/cpt.1166. doi:10.1002/cpt.1166.

15. Lorenzi M, Filippone M, Frisoni GB, Alexander DC, Ourselin S. Probabilistic disease progression modeling to characterize diagnostic uncertainty: Application to staging and prediction in Alzheimer's disease. *NeuroImage* 2017;(October):[in press]. doi:10.1016/j.neuroimage.2017.08.059.

25

16. Davatzikos C, Bhatt P, Shaw LM, Batmanghelich KN, Trojanowski JQ. Prediction of MCI to AD conversion, via MRI, CSF biomarkers, and pattern classification. *Neurobiology of Aging* 2011;32(12):2322.e19–27. URL: `http://www.pubmedcentral.nih.gov/articlerender.fcgi?artid=2951483{&}tool=pmcentrez{&}rendertype=abstract`. doi:10.1016/j.neurobiolaging.2010.05.023.

17. Moradi E, Pepe A, Gaser C, Huttunen H, Tohka J. Machine learning framework for early MRI-based Alzheimer's conversion prediction in MCI subjects. *NeuroImage* 2015;104:398–412. URL: `http://dx.doi.org/10.1016/j.neuroimage.2014.10.002`. doi:10.1016/j.neuroimage.2014.10.002. arXiv:15334406.

18. Long X, Chen L, Jiang C, Zhang L. Prediction and classification of Alzheimer disease based on quantification of MRI deformation. *PLoS ONE* 2017;12(3):1–19. doi:10.1371/journal.pone.0173372.

19. Lebedev AV, Westman E, Van Westen GJ, Kramberger MG, Lundervold A, Aarsland D, Soininen H, Kłoszewska I, Mecocci P, Tsolaki M, Vellas B, Lovestone S, Simmons A. Random Forest ensembles for detection and prediction of Alzheimer's disease with a good between-cohort robustness. *NeuroImage: Clinical* 2014;6:115–25. doi:10.1016/j.nicl.2014.08.023.

20. Wang T, Qiu RG, Yu M. Predictive Modeling of the Progression of Alzheimer's Disease with Recurrent Neural Networks. *Scientific Reports* 2018;8(1):1–12. URL: `http://dx.doi.org/10.1038/s41598-018-27337-w`. doi:10.1038/s41598-018-27337-w.

21. Mathotaarachchi S, Pascoal TA, Shin M, Benedet AL, Kang MS, Beaudry T, Fonov VS, Gauthier S, Rosa-Neto P. Identifying incipient dementia individuals using machine learning and amyloid imaging. *Neurobiology of Aging* 2017;59:80–90. doi:10.1016/j.neurobiolaging.2017.06.027.

22. Vogel JW, Vachon-Presseau E, Binette AP, Tam A, Orban P, Joie RL, Savard ML, Picard C, Poirier J, Bellec P, Breitner JCS, Villeneuve S. Brain properties predict proximity to symptom onset in sporadic Alzheimer's disease. *Brain* 2018;141:1871–83. URL: `http://adni.loni.usc.edu/wp-content/uploads/how{_}to{_}apply/ADNI{_}Acknowledgement{_}List.pdf{%}0Ahttps://academic.oup.com/brain/article-abstract/141/6/1871/4969934`. doi:10.1093/brain/awy093.

23. Rey A. L'examen psychologique dans les cas d'encéphalopathie traumatique. (Les problems.). [The psychological examination in cases of traumatic encepholopathy. Problems.]. *Archives de Psychologie* 1941;28:215–85.

24. Folstein MF, Folstein SE, McHugh PR. "Mini-mental state": A practical method for grading the cognitive state of patients for the clinician. *Journal of Psychiatric Research* 1975;12(3):189–98. doi:0022-3956(75)90026-6[pii].

25. Mohs RC, Knopman D, Petersen RC, Ferris SH, Ernesto C, Grundman M, Sano M, Bieliauskas L, Geldmacher D, Clark C, Thai LJ. Development of cognitive instruments for use in clinical trials of antidementia drugs: Additions to the Alzheimer's disease assessment scale that broaden its scope. *Alzheimer Disease and Associated Disorders* 1997;11(S2):S13–21.

26. Morris JC. The Clinical Dementia Rating (CDR): Current version and scoring rules. 1993.

27. Lewandowski D, Kurowicka D, Joe H. Generating random correlation matrices based on vines and extended onion method. *Journal of Multivariate Analysis* 2009;100(9):1989–2001. URL: `http://dx.doi.org/10.1016/j.jmva.2009.04.008`. doi:`10.1016/j.jmva.2009.04.008`.

28. Hoffman MD, Gelman A. The No-U-Turn sampler: Adaptively setting path lengths in Hamiltonian Monte Carlo. *Journal of Machine Learning Research* 2014;15:1593–623. URL: `http://arxiv.org/abs/1111.4246`. arXiv:`1111.4246`.

29. Salvatier J, Wiecki T, Fonnesbeck C. Probabilistic programming in Python using PyMC. *PeerJ Comput Sci* 2016;2(e55). URL: `http://arxiv.org/abs/1507.08050`. doi:`10.7717/peerj-cs.55`. arXiv:`1507.08050`.

30. Corder EH, Lannfelt L, Bogdanovic N, Fratiglioni L, Mori H. The role of APOE polymorphisms in late-onset dementias. *Cellular and Molecular Life Sciences* 1998;54(9):928–34. URL: `http://link.springer.com/10.1007/s000180050223`. doi:`10.1007/s000180050223`.

31. Younes L, Albert M, Miller MI. Inferring changepoint times of medial temporal lobe morphometric change in preclinical Alzheimer's disease. *NeuroImage: Clinical* 2014;5:178–87. URL: `http://www.pubmedcentral.nih.gov/articlerender.fcgi?artid=4110355{&}tool=pmcentrez{&}rendertype=abstract`. doi:`10.1016/j.nicl.2014.04.009`.

32. Iturria-Medina Y, Sotero RC, Toussaint PJ, Mateos-Perez JM, Evans AC, Initiative TADN. Early role of vascular dysregulation on late-onset Alzheimer's disease based on multifactorial data-driven analysis. *Nature Communications Commun* 2016;7:11934. URL: `http://dx.doi.org/10.1038/ncomms11934http://10.0.4.14/ncomms11934`. doi:`10.1038/ncomms11934`. arXiv:`arXiv:1011.1669v3`.

33. Bilgel M, Koscik R, An Y, Prince J, Resnick S, Johnson S, Jedynak B. Temporal order of Alzheimer's disease-related cognitive marker changes in BLSA and WRAP longitudinal studies. *Journal of Alzheimer's Disease* 2017;59(4):1335–47. doi:`10.3233/JAD-170448`.

34. Oxtoby NP, Garbarino S, Firth NC, Warren JD, Schott JM, Alexander DC. Data-driven sequence of changes to anatomical brain connectivity in

sporadic Alzheimer's disease. *Frontiers in Neurology* 2017;8:580. doi:`10.3389/fneur.2017.00580`.